JOURNAL OF CATALYSIS 36, 23–29 (1975)

Studies on Pore Structure of Adsorbents and Catalysts

I. Determination of the Pore Size Distribution of Synthetic Chrysotile by Electron Microscopy

J. J. F. SCHOLTEN, A. M. BEERS, AND A. M. KIEL*

Department of Chemical Technology, Delft University of Technology, Julianalaan 136, Delft-2208, The Netherlands

Received January 7, 1974

In order to obtain a preparation for checking the validity of the Kelvin equation for capillary condensation in cylindrical tubes of very small diameter, and the Washburn equation for mercury penetration in such tubes, the structure and texture of chrysotile and garnirite were studied by electron microscopy. A method is indicated by which the internal pore size distribution in such preparations can be calculated.

Garnirite is less suitable for the purpose, owing to unusual crystal growth and the occurrence of growth defects, but it lends itself excellently for visualizing by means of electron microscopy the layer structure of the walls of the hollow needles which form the crystallites in these asbestoslike silicates. The distance between the layers as established from electron microscopy is in rather good accordance with the distance determined crystallographically.

Pore size distributions are presented of chrysotile preparations as calculated from electron microscopy. In forthcoming publications these will be compared with distributions found from nitrogen capillary condensation and mercury porosimetry.

INTRODUCTION

Pore size distributions in adsorbents, catalysts, and other porous substances are generally determined by means of two techniques, viz. mercury penetration and capillary condensation of nitrogen (*1*). One of the difficulties encountered in the interpretation of the experimental results is that the form of the pores is mostly unknown, and in such cases one manages with an idealized pore model. In applying mercury penetration, for instance, a collection of perfectly cylindrical tubes open at both ends is chosen as a model. In reality, however, we are often dealing with a capricious mixture of pores of various shapes, which implies that the result of a pore size distribution analysis gives only an indistinct image of the real situation.

There is, however, a second difficulty which is often overlooked. Even if it is certain that the pores are cylindrical tubes open at both ends, the question arises whether the thermodynamic laws describing mercury penetration and nitrogen capillary condensation (the Washburn equation based on the equation of Young and Laplace, and the Kelvin equation (*1*)) may be applied to the very small pores present in most adsorbents and catalysts, where radii in the range 25–1000 Å are quite common.

The aim of the present series of articles is to present experimental results which can throw some light on this last question. For that purpose use was made of a porous compound possessing a curious morphology, viz. synthetic chrysotile, $Mg_3(OH)_4 \cdot Si_2O_5$, which consists of hollow needles of perfect cylindrical shape.

In the present article we describe the synthesis, structure and texture of chrys-

* Central Laboratory DSM, Geleen, The Netherlands.

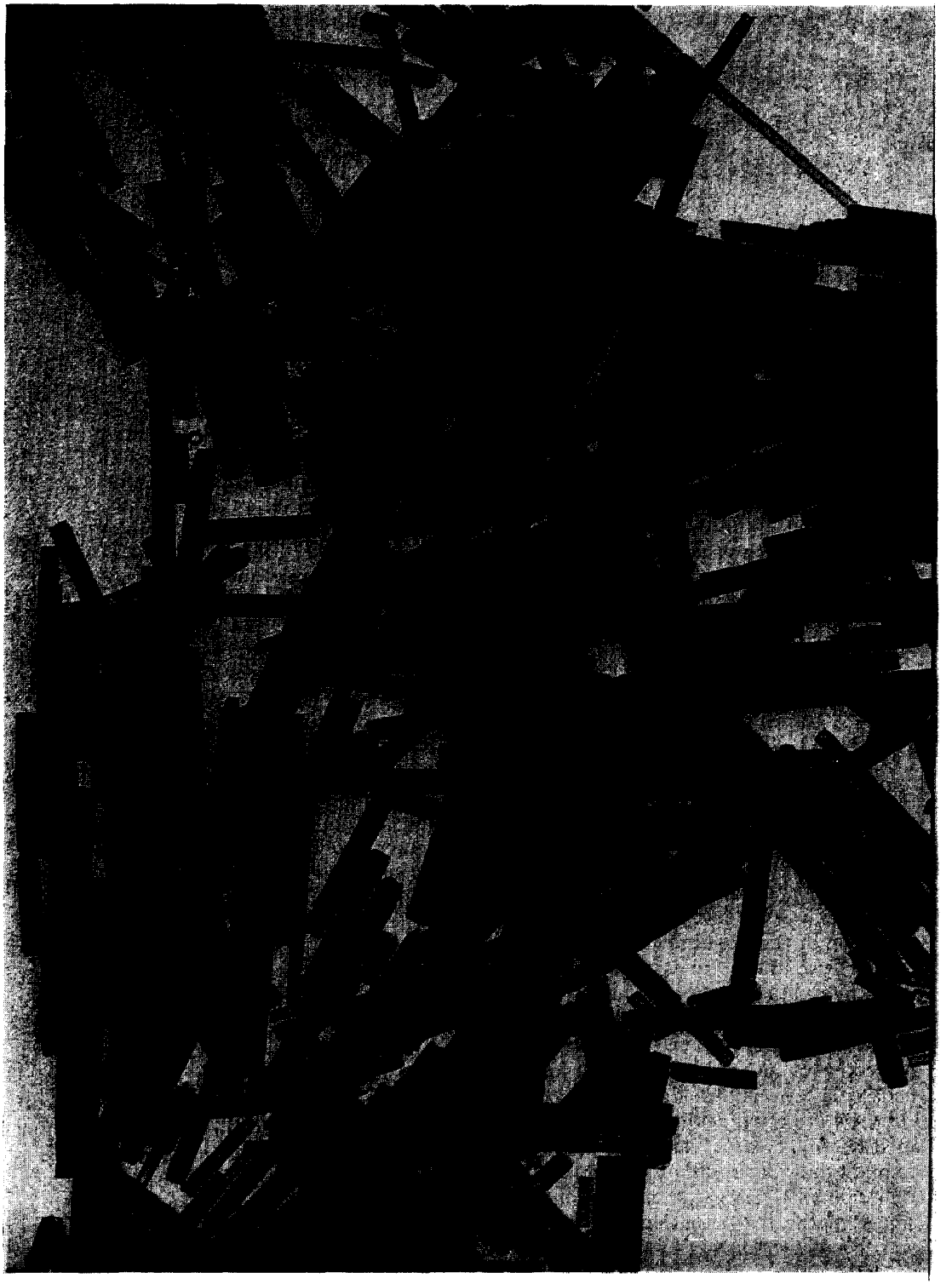

FIG. 1. Electron micrograph of synthetic chrysotile, $Mg_3(OH)_4 \cdot Si_2O_5$.

otile and its nickel isomorph garnirite, and the way in which the pore size distribution in the needles is determined from electron microscopy. The next article will deal with the theory of capillary condensation of liquid nitrogen in very narrow tubes of cylindrical shape, application of this theory to chrysotile, and comparison of the results with that found by electron microscopy. Finally, in a third article, we intend to discuss the penetration of mercury into chrysotile needles, and the corrections to be made to the Washburn equation in the case of very narrow pores.

Experimental

Chrysotile, $Mg_3(OH)_4 \cdot Si_2O_5$, was prepared according to the specifications by Noll, Kircher, and Sybertz (*2*). A solution of 102 g of $MgCl_2 \cdot 6H_2O$, reagent grade, in 200 cm³ of distilled water, was mixed with a solution of 95 g $Na_2Si_2O_3 \cdot 9H_2O$ prepared by dissolving silica (trade mark "Aerosil" of Degussa) in sodium hydroxide, and with 14 g sodium hydroxide, reagent grade, dissolved in 400 cm³ of distilled water. The quantities were so chosen as to correspond with the stoichiometry of chrysotile. The mixture was vigorously stirred, resulting in the precipitation of a white gellike substance. About 60 cm³ of the mixture was placed in a nickel crucible of 100 cm³ volume, which was mounted in a 1-liter autoclave filled with 400 cm³ of distilled water. After closing the autoclave, the temperature was raised to 295°C in 3 hr; the final steam pressure was then about 87 kg/cm². After 8 hr of reaction the autoclave was slowly cooled and opened. The gellike product was washed several times with distilled water to remove all of the chlorine, and subsequently with 96% ethanol. After evaporation of the alcohol at 100°C, the sample was dried at 110°C.

Garnirite, $Ni_3(OH)_4 \cdot Si_2O_5$, was prepared in a similar way, but magnesium chloride was replaced by nickel sulphate, reagent grade, from BDH.

Electron micrographs were taken with a Philips 300 M apparatus. Suspensions of chrysotile in alcohol were brought onto a small-mesh wire netting coated with a carbon film. Garnirite, embedded in methyl methacrylate was sectioned into coupes of less than 500 Å thickness. Lengths were calibrated by means of a Rowland grid of 2160 lines/mm.

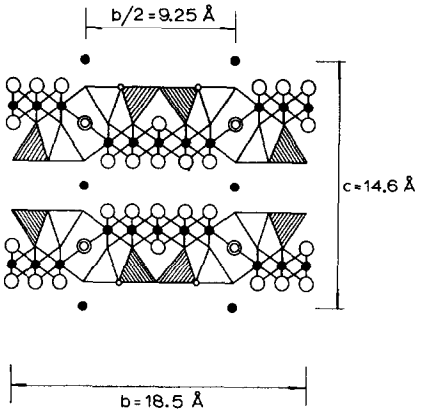

Fig. 2. Structure of chrysotile, according to Warren and Bragg (*3*). Projection in the direction of the X-axis, which is the axis of the chrysotile needle. Large circles, hydroxyl ions; small black circles, magnesium ions; double circles, water molecules; triangles, projection of the SiO_4 tetrahedra.

Results

Electron Microscopy

Figure 1 represents an electron micrograph of our chrysotile preparation, sample A. The hollow-needle shape of the crystallites is very evident. In some places where the needles are disposed perpendicularly to the plane of observation, the circular shape of the pores is clearly visible. Analogous micrographs were published earlier by Noll, Kircher, and Sybertz (*2*).

The crystallographic structure of chrysotile, as determined from X-ray diffraction by Warren and Bragg (*3*), is illustrated in Fig. 2. This figure pictures the atomic structure of the needle walls parallel to the needle axis. The walls are built up of spirally wound layers of $Mg_3(OH)_4 \cdot Si_2O_5$ which are spaced 7.3 Å apart and are interconnected by some of the magnesium ions.

The structure of garnirite is the same as that of chrysotile, the Mg^{2+} ions in Fig. 2 being replaced by Ni^{2+} ions. The isomorphism is bound up with the fact that the

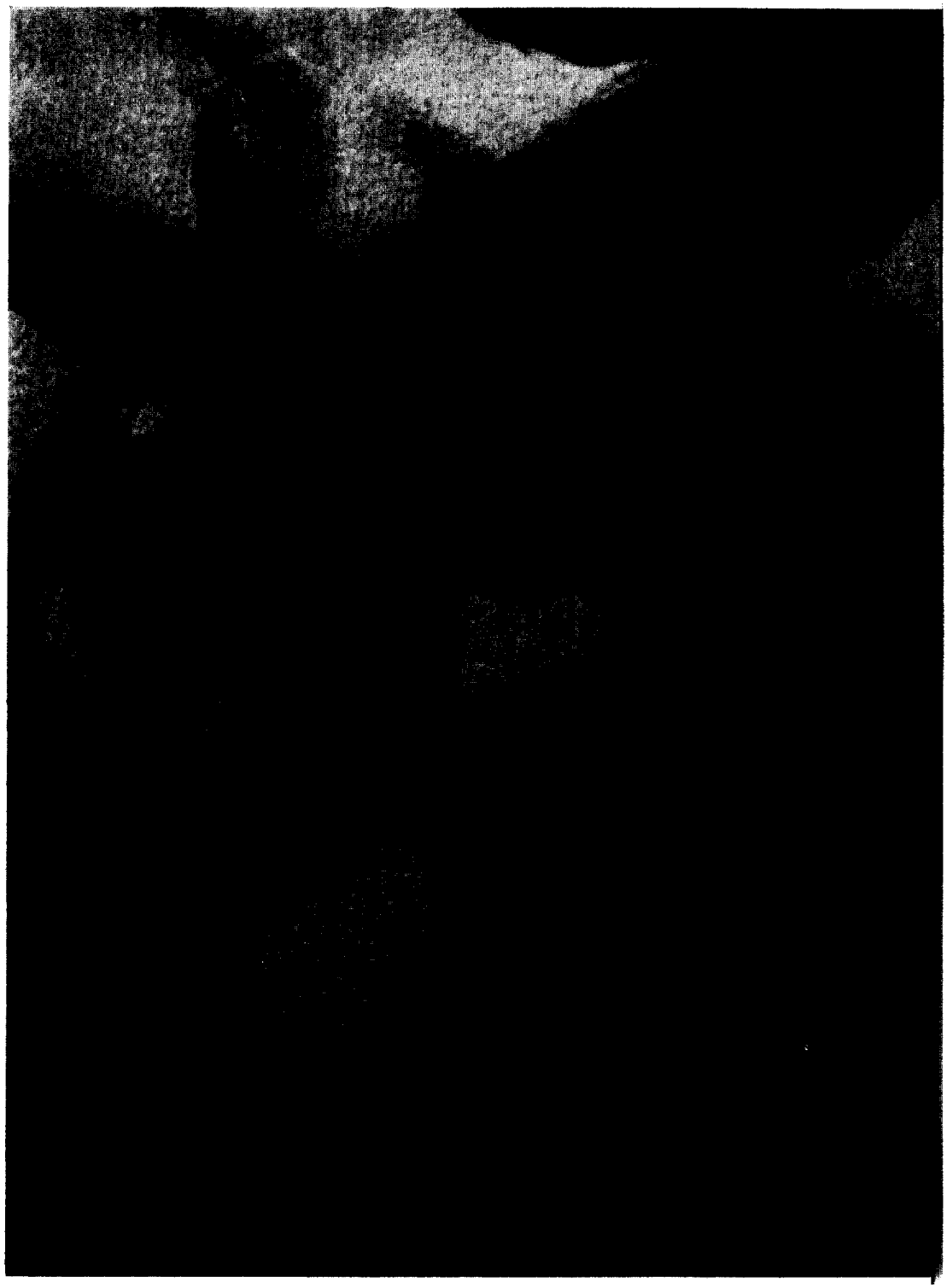

FIG. 3. Electron micrograph of a 500 Å microtome coupe of garnirite, $Ni_3(OH)_4 \cdot Si_2O_5$.

radii of the Ni^{2+} and Mg^{2+} ions are nearly equal, i.e., 0.68 and 0.65 Å, respectively.

In accordance with Noll and Kircher (*4*), our electron micrographs showed that the crystallites of garnirite have the same hollow-needle shape as chrysotile; however, unusual crystal growth and growth defects, as described for chrysotile–asbestos by Keiji Yada (*5*), were much more frequent than in the latter.

A high-resolution micrograph of garnirite (coupe technique) is presented in Fig. 3. The layer structure of the needle walls is now clearly visible, thanks to the scattering power being much higher for the 28 electrons of the Ni^{2+} ions than for the 10 electrons of the Mg^{2+} ions. From Fig. 3 we calculated the mean layer distance in the walls of the garnirite needles to be (7 ± 0.4) Å, a value which comes very near to the layer distance found crystallographically (7.3 Å). Keiji Yada (*5*) obtained a layer distance of 7.3 Å in natural chrysotile asbestos by high resolution electron microscopy.

Internal Pore Size Distribution in Synthetic Chrysotile

By means of a pocket lens we determined the internal and external radii and length of a large number of chrysotile needles in our micrographs, and constructed distribution diagrams on the basis of these countings. Table 1 gives the number averages of these quantities for our preparations A and B, as well as the results given by Noll, Kircher, and Sybertz (*2*), sample C. We see from the table that there exists a striking correspondence between the mean external and internal radii in preparations B and C, whereas the mean length of the needles varies quite strongly.

It is customary to represent pore size distributions by plotting the derivative of the internal pore volume with respect to the pore radius per unit weight, as a function of the pore radius. The calculation for all three samples was performed as follows. The mean mass $\bar{m}$ of one needle is given by

$$\bar{m} = \pi(\bar{r}_e^2 - \bar{r}_i^2)\bar{l}\ 2.6, \qquad (1)$$

2.6 being the specific mass of chrysotile (*2*). The mean value $\bar{m}$ will be very near to the number average of m, provided the distributions of r_e and r_i are independent of the distribution of l, and the standard deviations of $\bar{r}_e$ and $\bar{r}_i$ are much smaller than the standard deviation of $\bar{l}$. From an inspection of the distribution curves it appears that the distributions meet these requirements. Hence, the mass M of n needles counted is given by

$$M \simeq n\pi(\bar{r}_e^2 - \bar{r}_i^2)\bar{l}\ 2.6. \qquad (2)$$

The internal volume of a fraction of n_{r_i} needles of internal radius r_i is given by

$$V_{r_i} = n_{r_i}\pi r_i^2\bar{l}. \qquad (3)$$

From Eqs. (2) and (3) it follows that the internal volume of that fraction per unit weight is given by

$$V_{r_i}/M \simeq (n_{r_i}r_i^2)/[n(\bar{r}_e^2 - \bar{r}_i^2)2.6]. \qquad (4)$$

TABLE 1
CHARACTERISTIC NEEDLE DIMENSIONS IN THREE DIFFERENT CHRYSOTILE PREPARATIONS[a]

Sample	Number of needles counted (n)	Mean length of needles $\bar{l}$ (Å)	Mean internal radius of needles $\bar{r}_i$ (Å)	Mean external radius of needles $\bar{r}_e$ (Å)
(A) See Fig. 1, not used for further study	250	1712	32.2	141
(B) Used for further study	203	939	36.6	129
(C) Used by Noll *et al.* (*2*)	1000	1560	36.5	119.5

[a] Definitions: $\bar{l} = \Sigma l(n_l)/\Sigma n_l$, $\bar{r}_i = \Sigma r_i(n_{r_i})/\Sigma n_{r_i}$, $\bar{r}_d = \Sigma r_e(n_r)/\Sigma n_{r_e}$, $\Sigma n_i = \Sigma n_{r_i} = \Sigma n_{r_e} = n$. The standard deviations of $\bar{l}$, $\bar{r}_i$ and of $\bar{r}_e$ were about equal to the values found by Noll *et al.* (see the distribution curves in Ref. *2*).

TABLE 2

SAMPLE B. SPECIFIC INTERNAL PORE VOLUME (THIRD COLUMN), SPECIFIC CUMULATIVE INTERNAL PORE VOLUME (FOURTH COLUMN), AND THE DERIVATIVE OF THE CUMULATIVE INTERNAL PORE VOLUME TO THE PORE RADIUS (FIFTH COLUMN), FOR VARIOUS VALUES OF THE INTERNAL RADIUS (FIRST COLUMN)

r_i (Å)	n_{r_i}	V_{r_i}/M (cm³/g)	$\Sigma V_{r_i}/M$ (cm³/g)	$d\Sigma(V_{r_i}/M)/dr_i$ (cm³/gÅ)
65	1	5.23×10^{-4}	5.23×10^{-4}	$1\ .05 \times 10^{-4}$
60	1	4.46×10^{-4}	9.69×10^{-4}	0.89×10^{-4}
50	16	49.53×10^{-4}	59.22×10^{-4}	9.91×10^{-4}
45	15	37.61×10^{-4}	96.83×10^{-4}	7.52×10^{-4}
40	63	124.81×10^{-4}	221.64×10^{-4}	24.96×10^{-4}
35	37	56.12×10^{-4}	277.77×10^{-4}	11.22×10^{-4}
30	56	62.41×10^{-4}	340.17×10^{-4}	12.48×10^{-4}
25	11	8.51×10^{-4}	348.68×10^{-4}	1.70×10^{-4}
20	3	1.49×10^{-4}	350.17×10^{-4}	0.30×10^{-4}

Values of V_{r_i}/M for various groups of needles in preparation B, together with the internal volume of the needles per unit weight, and the derivative of this volume to the pore radius, are given in Table 2. In the calculations a group of needles of radius r_i was defined to be represented by all needles coming in the range of radii between $r_i - 2.5$ Å and $r_i + 2.5$ Å.

Figure 4 shows a plot of the pore size distribution for sample B. The distribution

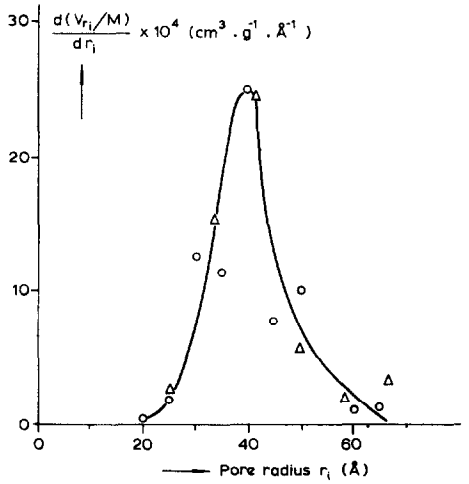

FIG. 4. Pore size distribution in synthetic chrysotile, as determined by electron microscopy. Open circles, preparation B; open triangles, preparation C. The solid line is drawn through the open circles. The position of the triangles shows that Noll *et al.* (*2*) arrived at practically the same distribution as that found in sample B.

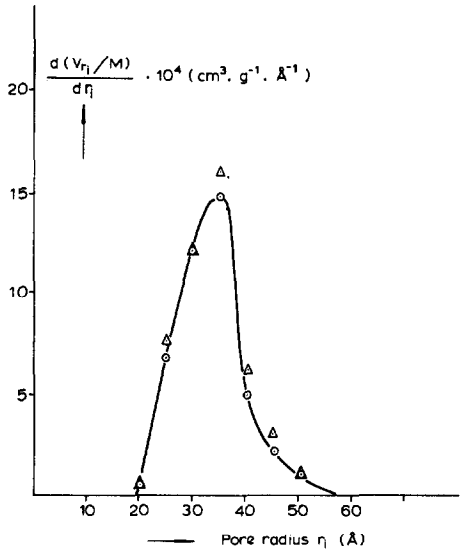

FIG. 5. Pore size distribution in synthetic chrysotile, as determined by electron microscopy, sample A. Open circles, calculated statistically; open triangles, calculated numerically.

in sample C, calculated from the distribution diagrams in the paper of Noll, Kircher, and Sybertz (*2*) is also included, and comparison reveals that the two distributions are practically equal.

Preparation A, which was not used for further study, clearly deviates in texture from samples B and C; $\bar{r}_e$ is significantly higher than for samples B and C, and $\bar{r}_i$ significantly lower; furthermore the peak in the distribution curve is situated at a value 4 Å smaller (see Fig. 5, open circles).

To find the extent to which the approximations made in the calculation of the mass M of n needles counted, from $\bar{m}$ in Eq. (1), are justified, an *absolute* calculation was carried out on sample A, taking into account the r_e, r_i and l values of each separate needle, and calculating from these values the whole distribution numerically. This resulted in the open triangle points in Fig. 5. One sees that the absolute calculation leads neither to a fundamentally different shape of the distribution curve, nor to a change in the position of the maximum of the curve, as compared with that of the curve through the open circles referring to the statistical calculation. However, the total pore volume found by integration of the curve is about 10% larger. Hence, we may conclude that the simple, faster calculation method applied to samples B and C satisfies our purpose.

Starting from the distribution curves a total surface area of 93 m^2/g was calculated for sample B, in quite good accordance with the measured BET surface area of 103 m^2/g (see Part II of this series). The inner surface area of the needles is 20% of the total surface area.

Discussion

Chrysotile is a useful starting material for checking the validity of the laws describing nitrogen capillary condensation and mercury penetration, at least in the area of pore radii around 40 Å. It is rather difficult to find materials having pores larger than 40 Å diameter and which are perfectly cylindrical throughout, but it might be that some natural asbestos materials whose internal radii come in a still somewhat higher range (*1*) would serve our purpose equally well.

Considering that our electron microscope was gauged by means of a Rowland grid, and that the EM and Röntgen values of the spacing between the layers forming the walls of the needles in garnirite exhibit good agreement, we feel that the pore size distributions found from EM observation may be regarded as "absolute" in the sense that the accuracy of the measured radii may be estimated to be about ±5%.

Searching for the cause to which the remarkable spiral growth of the needles is to be ascribed, we found that there may exist a wide variation in the internal radii, external radii and lengths of the needles in one and the same preparation, as well as in the mean values of these quantities in different preparations. It follows that the values of r_i and r_e are not, or only partly, determined by the crystallography of chrysotile. Therefore, we cannot agree with the explanation given by Noll and Kircher (*4*) who ascribed the spiral growth to a small difference in lattice constant between $Mg(OH)_2$ and Si_2O_5, which should cause bending of the plates. Moreover, their explanation conflicts with the crystallographic picture following from Bragg's work (Fig. 2) which revealed that the magnesium ions in the layers occur in a staggered arrangement on either side of the silica tetrahedra.

The explanation of Keiji Yada (*5*) appeals much more to us. This author states that the spiral growth is initiated by growth defects caused in the needle-wall plates owing to the presence of contaminating ions, or to the occurrence of dislocations. Once the first bend plate is closed, forming a cylinder, the needle wall will continue to grow in a spiral fashion, the connection between the layers being provided by a small portion of the magnesium ions (see Fig. 2).

Acknowledgments

Thanks are due to Dr. J. C. Rasser and to Mrs. L. de Wit for helpful discussions and mathematical assistance.

References

1. Thomas, J. M., and Thomas, W. J., *in* "Introduction to the Principles of Heterogeneous Catalysis." Academic Press, London and New York, 1967, pp. 195–212.
2. Noll, W., Kircher, H., and Sybertz, W., *Kolloid-Z.* **157,** 1 (1958).
3. Warren, B. E., and Bragg, W. L., *Z. Kristallogr. Kristallgeometrie Kristallphys. Kristallchem.* **76,** 201 (1930).
4. Noll, W., and Kircher, H., *Naturwissenchaften* **39,** 233 (1952).
5. Keiji Yada, *Acta Crystallogr.* **23,** 704 (1967).